Masson, L. ; Richards, B.S. ; Schäfer, A. I. (2005) System design and performance testing of a hybrid membrane-photovoltaic desalination system, Desalination, 179, 61-69
doi:10.1016/j.desal.2004.12.022

# System Design and Performance Testing of a Hybrid Membrane – Photovoltaic Desalination System

[1,2] Laurent Masson [3] Bryce S. Richards, [1*] Andrea I. Schäfer

[1] *Environmental Engineering, University of Wollongong, Wollongong, NSW 2522, AUSTRALIA*
[2] *ESIGEC, Université de Savoie, Le Bourget du Lac, 73376, FRANCE*
[3] *Centre of Excellence for Advanced Silicon Photovoltaics and Photonics, University of New South Wales, Sydney, NSW 2052, AUSTRALIA*
**corresponding author schaefer@uow.edu.au, ph +61 2 4221 3385, +61 2 4221 4738*

## Abstract

In some areas limited water resources combined with the fast growing population are leading to a crucial situation because of the increase in water demand. Besides, an estimated one billion people are living both without access to clean drinking water or electricity. Therefore, a stand alone photovoltaic-power based hybrid membrane desalination prototype has been designed to meet this challenge. Several parameters were examined in order to optimise the system performance, including i) feed water salt concentration, ii) operating pressure, iii) system recovery, iv) specific energy consumption (SEC) and v) salt retention. With a SEC varying from 2.2 to 7.7 kWh.m$^{-3}$, the installation designed for remote villages is able to produce up to 1.2 m$^3$.d$^{-1}$.

*Keywords:* Desalination, Reverse Osmosis, Nanofiltration, Photovoltaic, Remote Community Water Supply

## 1. Introduction

The lack of water resources and safe drinking water scarcity has been recognized and analysed by different international organisations such as the World Health Organisation or the World Bank [1]. The problem is being further deteriorated by the pollution of the rivers and lakes from industrial waste and sewage discharge. On a global scale, man-made pollution of natural resources of water is becoming the single largest cause for the fresh water shortage [2].

Further, the lack of adequate treatment facilities leads to adverse health effects for local community members especially in rural and remote areas. While the remote conditions make it rather difficult to operate and maintain conventional treatment technology, its application is often limited by the availability of electricity, with many rural areas having no access to a national electricity grid. Therefore, it is widely recognised that water filtration methods powered by renewable energy sources are needed around the world [3].

In response to this need, several photovoltaic (PV) powered reverse osmosis (RO) and other such water desalination and filtration systems do exist to tackle water shortages [4-12]. The adaptation of such systems to remote community use, where maintenance facilities are generally not available, is largely a question of system design.

This led to the development of a photovoltaic-powered reverse osmosis desalination unit, called ROSI (Reverse Osmosis Solar Installation), which is designed to deliver a production flow of 1 000 L per day of clean drinking water from various ground or surface water sources to meet the demand of a small remote community.

## 2. Review of existing PV powered membrane filtration systems

PV-powered water pumping systems are extremely reliable, and are able to provide water in remote areas for the lowest costs [5]. Consequently, many examples of photovoltaic powered reverse osmosis (PV-RO) treatment systems can be found in the literature. The majority of PV-RO systems have been designed to operate at high pressures (> 40 bar) in order to desalinate seawater, often for off-shore applications. An overview of PV-RO systems reported in the literature, including various operating parameters and system performance is shown in Table 1.

**Table 1: Overview of PV-RO units sorted by PV array size (adapted from [6])**

| Location | TDS Conc. (g.L$^{-1}$) | $P_{operate}$ (bar) | Salt Retention (%) | Recovery (%) | Clean Water (m$^3$.d$^{-1}$) | SEC (kW.h.m$^{-3}$) |
|---|---|---|---|---|---|---|
| Portugal | 2-5 | 4 | 90 | 2 | 0.02 | 25.6 |
| Australia | 3.5 | 4-10 | 92 | 10 | 0.1 | 8 |
| Australia | 5 | - | - | 16 or 25 | 0.4 | - |
| Canada | 33 | 34-35 | 97-99 | 14 | 0.85 | 4.0 |
| Australia | - | - | 88 | - | 0.4-1.0 | 4.0-5.8 |
| UK | 40 | 40-60 | - | - | 3[†] | 3.5[†] |
| Mexico | Brackish | 40 | - | - | 0.7-1.4 | 4.0-6.9 |
| Oman | 1 | 12 | 96.6 | 65-70 | 5 | 2.3 |
| Israel | 4 | 4-16 | 98 | 50 | 3 | - |
| Spain | 35 | 45-70 | >98.5 | - | >0.8 | 15-16 |

[†] *Simulated results*

The limitation of many systems is membrane fouling which needs to be addressed with appropriate pre-treatment methods. To date such pre-treatment as well as long term system maintenance methodologies have not been fully explored.

## 3. System design

### *3.1. Main concept and history of the project*

The basic design concept for the reverse osmosis solar installation (ROSI) is to use a photovoltaic powered source to power pumps required to produce the driving force for the hybrid membrane process to produce potable water from a variety of possible water sources (from high turbidity surface waters to high salinity brackish water). For the various prototypes developed an operating window is determined where SEC is acceptable and water quality produced meets drinking water guidelines.

The first stage is an ultrafiltration (UF) membrane, which serves as a pre-treatment step for the following stage, a reverse osmosis (RO) or nanofiltration (NF) membrane. The UF membrane removes most pathogens like bacteria as well as particles and some colloidal material (such as viruses or metal oxides), thus protecting the RO/NF membrane from excessive fouling, in particular biofouling, and hence reducing the required cleaning frequency of these modules. The RO/NF membrane retains ionic species and organic material, decreasing salinity and the concentration of harmful trace contaminants (e.g. F, As, B, $NO_3$, U) as well as dissolved organic matter. A basic diagram of the ROSI system is shown in Figure 1and a picture of the current system in Figure 2.

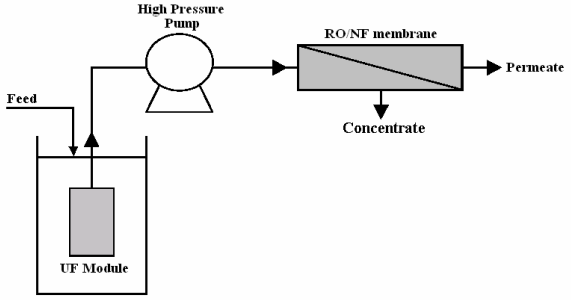


**Figure 1: Schematic diagram of the membrane configuration of prototype III.**

Masson, L. ; Richards, B.S. ; Schäfer, A. I. (2005) System design and performance testing of a hybrid membrane-photovoltaic desalination system, Desalination, 179, 61-69
doi:10.1016/j.desal.2004.12.022

**Figure 2: Picture of prototype III.**

Further design requirements result from the projected application of the system in remote communities. The system has to be robust, almost maintenance free, modular in size to fit a wide range of water demands, and it must be able to perform stand-alone operation. Concerning the product quality, the system has to be capable of reliably removing salinity, trace contaminants as well as pathogens to meet the requirements for clean and healthy drinking water.

### *3.2. Membrane selection*

Pre-treatment UF membranes: because it allows removing suspended solids and colloidal materials completely and reliably without chemicals addition, ultrafiltration (UF) is an ideal pre-treatment method for Reverse Osmosis [7]. Therefore, six submerged ultrafiltration modules, Zenon™ ZeeWeed 10 were selected for the pre-treatment process. The membranes have, according to the manufacturer, a nominal pore diameter of 0.4 µm, an effective membrane surface area of 0.93 $m^3$ per module, an operating pressure range of 0.07-0.55 bar, a typical permeate flow of 0.7 $L.min^{-1}$ and are operated in outside-in configuration. The UF is operated with a suction pressure by the high pressure pump.

Desalination RO/NF membranes: the design of a system fulfilling the remote area criteria [13] depends upon sacrificing high efficiency in terms of permeate flux, high recovery, salt rejection and operating pressure, with benefits of lower fouling incidence, low or no brine production and lower total energy input requirements [8]. Besides, the selection of an appropriate RO/NF membrane depends also on the feed water quality and targeted contaminants that have to be retained. Consequently, the choice of the RO/NF membrane is crucial, but water quality (and hence location) dependent.

In this project, two different membrane types have been tested with the system to identify the optimum membrane choice for different feed waters. Two different low-pressure RO/NF membranes were selected (Dow™ FilmTec NF90-4040 and Dow™ FilmTec BW30-4040). They have high sodium chloride retention and can be operated at low transmembrane pressure (typically 4-10 bar). Some of the module specifications are given in Table 2.

**Table 2: Selected RO/NF membrane characteristics (courtesy of DOW™ technical information)**

| Product | Description | Diameter inches (mm) | Element Size Length inches (mm) | Active Surface Area sq ft ($m^2$) | Flow gpd ($m^3.d^{-1}$) | Stabilized Rejection % |
|---|---|---|---|---|---|---|
| FILMTEC NF90-4040 | Nanofiltration element | 3.9 (99) | 40 (1 016) | 72 (6.7) | 2 200 (8.3) | 95.0 |
| FILMTEC BW30-4040 | Brackish water Reverse Osmosis membrane elements | 3.9 (99) | 40 (1 016) | 82 (7.6) | 2 400 (9.1) | 99.5 |

### *3.3. High pressure pump*

The high-pressure pump is a LowFlow LF 502 pump provided by Mono™. This progressive cavity pump delivers a maximum flow of 470 $L.h^{-1}$ at 15 bar pressure. When grid powered, it has a flat performance curve, resulting in a small drop in maximum flow rate (about 1.5%) when operating at high pressure compared to low-pressure operation. This pump suits PV applications since the motor automatically switches on as soon as power is supplied. The speed of the motor and thus the flow rate will increase or decrease as the solar radiation levels increase or decrease.

### *3.4. Solar power*

At the present stage, the system is running on grid power (through a 0-180V DC power supply) to enable testing of different components and optimising operating parameters under constant power conditions. However, the technologies chosen for the full-scale design are suitable for running on solar power. This option will be introduced as soon as the power requirements of the new system design are determined and the PV array can be sized accordingly.

## 4. Materials & Methods

### *4.1. Feed solution preparation and concentration*

Salt concentrations in a range of 0.5 to 35 $g.L^{-1}$ were used to cover the range of potable water sources from drinking water quality to seawater and determine system limitations. A 200 L plastic drum was used as a feed tank. It was filled with tap water, and swimming pool salt (Sunray Swimming Pool Salt™, CHEETHAM Salt Limited) was added to adjust the salt concentration (e.g. to adjust a salt concentration of 5 $g.L^{-1}$, 1 000 g of pool salt were added).

**Table 3: Composition of pool salt (5 $g.L^{-1}$ solution of sample analysed).**

| Salt | Concentration ($mg.L^{-1}$) | Mass fraction (%) |
|---|---|---|
| Sodium | 1979 | 40 |
| Calcium | 2.4 | 0.05 |
| Potassium | 1.8 | 0.05 |
| Magnesium | 0.6 | - |
| Iron | 0.01 | - |
| Chloride | 2754 | 55 |
| Sulfate | 6 | 0.1 |
| Total Hardness (as $CaCO_3$) | 9 | - |
| Boron | <0.10 | - |
| Fluoride | <0.10 | - |
| Nitrate | <1 | - |

Masson, L. ; Richards, B.S. ; Schäfer, A. I. (2005) System design and performance testing of a hybrid membrane-photovoltaic desalination system, Desalination, 179, 61-69
doi:10.1016/j.desal.2004.12.022

*4.2. Analytical methods*

Water samples were analysed using a WTW™ universal meter (model MultiLine P4), which measures conductivity, temperature and pH. The salt concentration of the steams were estimated using the measured conductivity values and a measured calibration curve for the pool salt (conductivity ($mS.cm^{-1}$) = 1.55 salt concentration ($g.L^{-1}$). This method assumes the same salt composition in each sample and hence neglects the varying retention for different salts by the membranes. The resulting error is expected to be low, however, seeing that 95% of the pool salt is in fact NaCl (see Table 3).

*4.3. Testing protocol and determination of performance indicators*

The set of experiments presented in this paper consisted of monitoring the performance of the system as a function of the feed flow rate and a constant operating pressure. Before the first measurement in each experiment, the system was run for at least 15 minutes to stabilise the performance of the membrane and to bleed air trapped in the system. The operating pressure of the RO/NF module was then set to 10 bar by adjusting the needle valve of the concentrate stream. Both the permeate and the concentrate were recycled back into the feed tank to maintain a stable feed concentration, and the water samples were returned to the feed tank after analysis for conductivity, temperature and pH. During each experiment, a number of key parameters of the installation were measured (permeate flow rate [$L.h^{-1}$], concentrate flow rate [$L.h^{-1}$], transmembrane pressure [bar]) and performance indicators calculated as specified in equations (1) to (4).

$$\text{System recovery } Y = \frac{Q_P}{Q_F} \times 100 \ [\%] \qquad (1)$$

$$\text{Salt retention } R = \left(1 - \frac{C_P}{C_F}\right) \times 100 = \left(1 - \frac{\text{Conductivity}_{\text{permeate}}}{\text{Conductivity}_{\text{feed}}}\right) \times 100 \ [\%] \qquad (2)$$

$$\text{Power consumption } P = I\,(\text{Ampere}) \times U\,(\text{Volt}) \ [\text{W}] \qquad (3)$$

$$\text{Specific energy consumption } SEC = \frac{P}{Q_p} \ [\text{W.h.L}^{-1}] \qquad (4)$$

Both permeate and concentrate flow rates were determined using a measuring cylinder and a stopwatch. The feed flow rate was calculated as the sum of permeate and concentrate flow rate (single pass configuration as shown in Figure 1). The power requirement of the system was recorded using two Digitech™ multimeters (model QM-1526).

## 5. System Optimisation: Results and Discussion

Permeate flux, specific energy consumption, salt retention and recovery are the most important performance indicators. In this study flux, SEC and retention were determined for different membranes as a function of recovery. To set different recoveries the system pressure was set at 10 bar and flowrates changed to achieve the desired recovery values. The values for both membranes relating flow rate and recovery are shown in Table 4.

**Table 4: Recovery of NF90 and BW30 membrane as a function of feed flowrate at constant pressure operation (10 bar, Salt conc. 5 $g.L^{-1}$)**

| **Feed Flow rate ($L.h^{-1}$)** | 150 | 200 | 250 | 300 | 350 | 400 | 450 | 500 |
|---|---|---|---|---|---|---|---|---|
| **NF90 recovery (%)** | 53 | 45 | 43 | 38 | 37 | 36 | 33 | 31 |
| **BW30 recovery (%)** | 38 | 33 | 27 | 25 | 24 | 23 | 21 | 19 |

Results for the NF 90 and BW 40 membranes are shown in Figure 3 and Figure 4, respectively. Permeate flux is highest for the lowest feed flow rate where the permeate flux decreases because the flow has to be restricted with the needle valve in order to achieve the operating pressure of 10 bar. Another reason for the high recovery values can be found in the system configuration: the positive displacement pump is not capable of maintaining the high feed flow due to a trade-off of voltage (~flow) for current (~pressure). Ideally, the feed flow rate would be constant to maintain a high cross-flow velocity and prevent excessive concentration polarisation caused by the high recovery. However, in reality when the system would be operated with variable sunpower, the power would constantly fluctuate and it is hence important to examine the system at all possible operating conditions.

As expected, the permeate fluxes obtained with the RO membrane (BW30) are lower than the ones obtained with the NF membrane (NF90) which was predictable since the calculated resistance of the RO membrane (≈ $6.10^{15}$ $m^{-1}$) is higher than the calculated resistance of the NF membrane (≈ $10^{14}$ $m^{-1}$) resulting thus in a lower permeate flux for the same applied pressure (see Table 5).

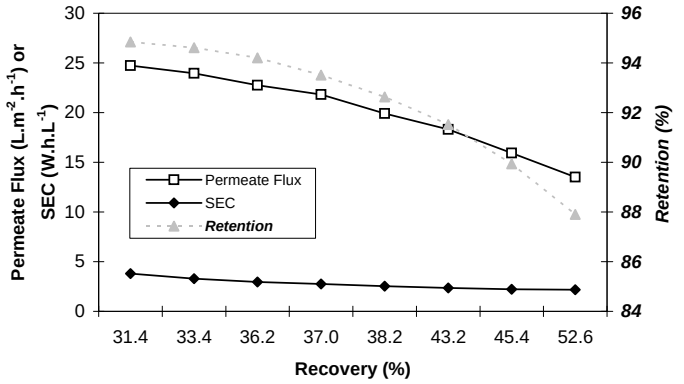


**Figure 3: Permeate flux, SEC, and retention as a function of recovery for NF90 membrane (feed temperature = 15 °C, conductivity = 8.21 $mS.cm^{-1}$, [Pool salt] = 5 $g.L^{-1}$, pH = 7.2)**

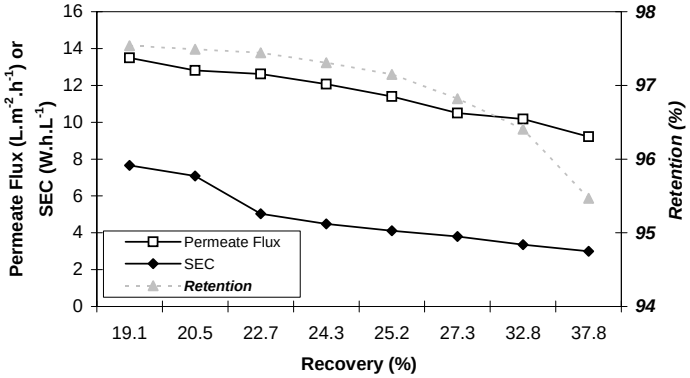


**Figure 4: Permeate flux, SEC, and retention as a function of recovery for BW30 membrane** (feed temperature = 14 °C, conductivity = 8.21 $mS.cm^{-1}$, [Pool salt] = 5 $g.L^{-1}$, pH = 7.5)

Masson, L. ; Richards, B.S. ; Schäfer, A. I. (2005) System design and performance testing of a hybrid membrane-photovoltaic desalination system, Desalination, 179, 61-69
doi:10.1016/j.desal.2004.12.022

**Table 5: Permeate flux comparison between BW30 and NF90 membranes at varying feed flowrates and recovery (10 bar, salt concentration 5 g.L$^{-1}$)**

| Feed flow rate (L.h$^{-1}$) | 150 | 200 | 250 | 300 | 350 | 400 | 450 | 500 |
|---|---|---|---|---|---|---|---|---|
| BW30 permeate flux compared to NF90 | 31.7 % lower | 36.2 % lower | 42.7 % lower | 42.7 % lower | 44.7 % lower | 44.5 % lower | 46.5 % lower | 45.4 % lower |

The salt retention is increasing when recovery increases (lower feed flow rate). One explanation is the effect of concentration polarisation due to higher recovery and lower cross-flow velocity. This leads to a high concentration of rejected ions near the membrane surface, subsequently developing a high concentration gradient from the concentrate side to the permeate side of the membrane. This gradient increases diffusion of ions across the membrane into the permeate stream, resulting in a lower salt retention. Especially the small monovalent ions ($Na^+$, $Cl^-$) are likely to pass the membrane by diffusion [14]. This phenomenon becomes most obvious at the higher recoveries. Table 6 illustrates the fact that the RO membrane (BW30) is only slightly more efficient than the NF membrane (NF90).

**Table 6: Comparison of retention between BW30 and NF90 membranes at varying feed flowrates and recovery (10 bar, salt concentration 5 g.L$^{-1}$)**

| Feed flow rate (L.h$^{-1}$) | 150 | 200 | 250 | 300 | 350 | 400 | 450 | 500 |
|---|---|---|---|---|---|---|---|---|
| BW30 retention compared to NF90 | 8.6 % higher | 7.2 % higher | 5.8 % higher | 4.9 % higher | 4.1 % higher | 3.4 % higher | 3 % higher | 2.8 % higher |

However, when presenting the results as permeate concentration (see Figure 5) the difference between the two membranes highlights that only the RO membrane is able to produce water that meets the Australian Drinking water guidelines at the low feed flow rates and high recoveries (with a feed salt concentration of 5 g.L$^{-1}$). For the NF90 membrane recoveries lower than 45% are required to maintain the water quality requirement. At higher salt concentrations the water quality will be more limiting.

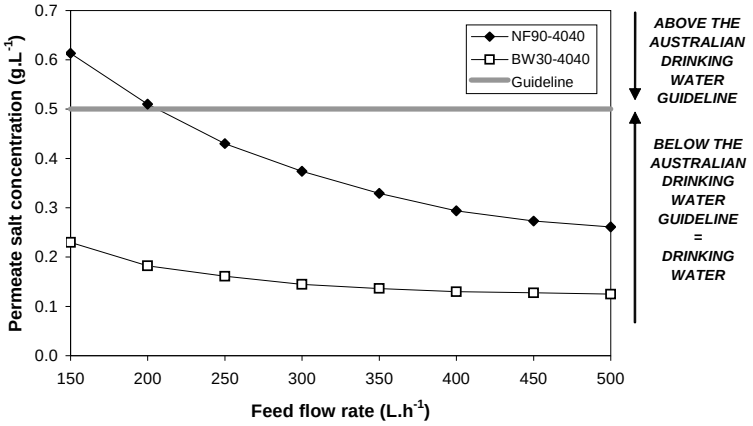


**Figure 5: Permeate salt concentration vs. feed flow rate at varying feed flowrates and recovery (10 bar, salt concentration 5 g.L$^{-1}$, feed temperature = 15 °C, conductivity = 8.21 mS.cm$^{-1}$, [Pool salt] = 5 g.L$^{-1}$, pH =7.2)**

The specific energy consumption is the energy required per unit of clean water produced and indicates the energy efficiency of the water treatment system. This is an important design attribute, especially when operating off a stochastic power source. To optimise the energy efficiency, the SEC can be minimised by either varying the operating conditions (e.g. pressure) or the system configuration (e.g. pump, option of energy recovery). Energy requirements depend on recovery, transmembrane pressure and hence salt concentration. As demonstrated in Figure 3 and Figure 4 the SEC increases with increasing feed flow rate from 2.2 to 7.7 kWh.m$^{-3}$ at a feed concentration of 5 g.L$^{-1}$ salt depending on the type of membrane in use. The membranes are compared in As shown in Table 7, the SECs with the RO membrane (BW30) are higher than with the NF membrane (NF90) since the resistance of the membrane is higher, resulting in lower permeabilities (lower water productivity) and hence higher energy requirement.

**Table 7: SEC comparison between BW30 and NF90 membranes at varying feed flowrates and recovery (10 bar, salt concentration 5 g.L$^{-1}$)**

| Feed flow rate (L.h$^{-1}$) | 150 | 200 | 250 | 300 | 350 | 400 | 450 | 500 |
|---|---|---|---|---|---|---|---|---|
| BW30 SEC compared to NF90 (%) | 38 % higher | 52 % higher | 61 % higher | 62 % higher | 63 % higher | 70 % higher | 115 % higher | 102 % higher |

## 6. Conclusions

The PV-powered hybrid membrane treatment system described in this paper has demonstrated good performance over a wide operating range. This stand-alone treatment system, based on a two-stage membrane filtration process, with six submerged ultrafiltration modules as a pretreatment stage and a RO/NF module for desalination and trace contaminant removal, can be used for different types of feed waters. Its robust, simple and almost maintenance-free technology makes it suitable for application in remote communities.

The specific energy consumption (SEC) varied from 2.2 to 7.7 kWh.m$^{-3}$ at a feed salt concentration of 5 g.L$^{-1}$ at an operating pressure of 10 bar depending on the type of membrane in use. The SEC decreases until permeate flow drops due to salinity limitations at high recoveries.

On the whole, the results of the performance testing show that the pump limitations of prototype II have been overcome and will lead to further system optimisation regarding design and operation of the prototype. Additional research is in progress to evaluate the long-term performance of the system (e.g. considering fouling and cleaning of the membranes), to optimise the energy efficiency to reduce initial costs and to assess the performance in terms of trace contaminants removal.

## 7. Acknowledgements

Andrew Moore and Paul Jeffery from Mono Australia are thanked for their continuous support and their pump expertise. Dow Chemicals it acknowledged for the provision of membrane modules. A scholarship from the Region Rhône-Alpes, France for the first author is much appreciated. Project funding was provided by the Australian Research Council (ARC) under the Linkage scheme (project number LP0349322). Ian Laird and Norm Gal are thanked for their technical support for the project in the Fluids Laboratory at UoW and Christian Remy (TU Berlin, Germany) for his design of the ROSI prototype III during his practicum at UoW in 2002/3.

## 8. References

1. Thomas, J.S. and Durham, B., Integrated water resource management: looking at the whole picture. Desalination, 2003. 156: p. 21-28.
2. Malik, M.A.S., Tiwari, G.N., Kumar, A., and Sodha, M.S., Solar desalination, in Pergamon press 1985.
3. Joyce, A., Loureiro, D., Rodrigues, C., and Castro, S., Small reverse osmosis units using PV systems for water purification in rural places. Desalination, 2001. 137: p. 39-44.
4. Herold, D., Horstmann, V., Neskakis, A., and Plettner-Marliani, J., Small scale photovoltaic desalination for rural water supply demonstration plant in Gran Canaria. Renewable Energy, 1998. 14(1-4): p. 293-298.

Masson, L. ; Richards, B.S. ; Schäfer, A. I. (2005) System design and performance testing of a hybrid membrane-photovoltaic desalination system, Desalination, 179, 61-69
doi:10.1016/j.desal.2004.12.022

5. Cartwright, P.S., Membrane separation technologies - practical applications, International Symposium on Safe Drinking Water in Small Systems: Technology, Operations, and Economics, Washington D.C., CRC Press LLC, 1998.
6. Richards, B.S., Remy, C., and Schäfer, A.I., Sustainable drinking water production from brackish sources using photovoltaics, 19th European Union Photovoltaics and Solar Energy Conference, Paris, 2004.
7. Côté, P., Cadera, J., Coburn, J., and Munro, A., A new immersed membrane for pretreatment to reverse osmosis. Desalination, 2001. 139: p. 229-236.
8. Robinson, R., Ho, G., and Kuruvilla, M., Development of a reliable low-cost reverse osmosis desalination unit for remote communities. Desalination, 1991. 86: p. 9-26.
9. Swinton, E.A., Developments in appropriate water treatments technologies., Science and Technology for Aboriginal development, Commonwealth Scientific and Research Organisation, Melbourne, 1985.
10. Thomson, M., Miranda, M.S., and Infield, D., A small-scale seawater reverse-osmosis system with excellent energy efficiency over a wide operating range. Desalination, 2002. 153: p. 229-236.
11. Gotor, A.G., Pestana, I.D.l.N., and Espinoza, C.A., Optimization of RO desalination systems powered by renewable energies. Desalination, 2003. 156: p. 351.
12. Bouchekima, B., Solar desalination plant for small size use in arid areas of South Algeria for the production of drinking water. Desalination, 2003. 156: p. 353-354.
13. Robinson, R., Ho, G., Mathew, K., Development of a reliable low-cost reverse osmosis desalination unit for remote communities. Desalination, 1991. 86: p. 9-26.
14. Williams, M.E., A review of reverse osmosis theory, Williams Engineering Services Company, Inc., 2003.